Joint International Topical Meeting on Mathematics & Computation and Supercomputing in Nuclear Applications (M&C + SNA 2007)
Monterey, California, April 15-19, 2007, on CD-ROM, American Nuclear Society, LaGrange Park, IL (2007)

SINGULAR CHARACTERISTIC TRACKING ALGORITHM FOR IMPROVED SOLUTION ACCURACY OF THE DISCRETE ORDINATES METHOD WITH ISOTROPIC SCATTERING

Jose I. Duo and Yousry Y. Azmy
The Pennsylvania State University
138 Reber Building, University Park, PA 16802
jid114@psu.edu; yya3@psu.edu

ABSTRACT

A new method, the Singular Characteristics Tracking algorithm, is developed to account for potential non-smoothness across the singular characteristics in the exact solution of the discrete ordinates approximation of the transport equation. Numerical results show improved rate of convergence of the solution to the discrete ordinates equations in two spatial dimensions with isotropic scattering using the proposed methodology. Unlike the standard Weighted Diamond Difference methods, the new algorithm achieves local convergence in the case of discontinuous angular flux along the singular characteristics. The method also significantly reduces the error for problems where the angular flux presents discontinuous spatial derivatives across these lines. For purposes of verifying the results, the Method of Manufactured Solutions is used to generate analytical reference solutions that permit estimating the local error in the numerical solution.

Key Words: Discrete Ordinates; Local Convergence; Nodal Methods; Manufactured Solution.

1. INTRODUCTION

Convergence of a numerical method's solution to the exact solution has long been established as a useful measure to estimate the accuracy of the discretization approximations and provide fundamental means to improve their performance. In particular, we are concerned with the spatial approximations to numerically solve the steady state one speed Discrete Ordinates (DO) equation

$$\hat{\Omega}_i \cdot \nabla \psi(\vec{x},\hat{\Omega}_i) + \sigma(\vec{x})\psi(\vec{x},\hat{\Omega}_i) = \sigma_s(\vec{x})\sum_{n=1}^{N} w_n \psi(\vec{x},\hat{\Omega}_n) + Q(\vec{x},\hat{\Omega}_i) \qquad (1)$$

where

$\psi(\vec{x},\hat{\Omega}_i)$ is the angular flux,

$\hat{\Omega}_i = (\mu_i,\eta_i,\varsigma_i)$ is the discrete ordinate (direction) unit vector,

$\sigma(\vec{x})$ and $\sigma_s(\vec{x})$ are the total and isotropic scattering macroscopic cross sections

$\phi(\vec{x}) = \sum_{n=1}^{N} w_n \psi(\vec{x},\hat{\Omega}_n)$ is the scalar flux computed with angular quadrature weights $\sum_{n=1}^{N} w_n = 1$

$Q(\vec{x},\hat{\Omega}_i)$ is the external fixed source.

Previous studies by Arkuszewski [1] numerically showed that, for point difference schemes of the DO equation, the convergence rate of the error's supremum norm is considerably worse than the L_2 norm for problems whose exact solution possesses discontinuous derivatives. Later, he devised a point scheme that preserves second order of convergence in the case of exact solution with discontinuous first derivative [2]. In the case of discontinuous exact angular flux, a local error analysis [4] has demonstrated that, for Weighted Diamond Difference (WDD) methods, the error does not vanish in the limit of diminishing cell size. This occurs, in particular, when boundary fluxes on the incoming faces are not equal resulting in a S*ingular Characteristic* (SC) across which the solution is discontinuous. Global error analysis of the same class of numerical methods was also performed in the context of Larsen's benchmark problem that employs a non-scattering medium [8], thus verifying the results of the local error analysis described above.

To raise the rate of convergence and significantly reduce the error for the case of discontinuous exact flux, the *Singular Characteristic Tracking* (SCT) algorithm is proposed. Unlike the point methods considered earlier [2], the SCT is based on a standard cell–balance formulation that explicitly imposes conservation of particles. In this paper we extend the results presented in [6] where local convergence was demonstrated for the uncollided flux in configurations with discontinuous exact solutions using the Singular Characteristic Tracking algorithm, whereas standard discretization schemes fail to converge locally. Here, error norms and their rate of convergence for problems with isotropic scattering are illustrated in two-dimensional Cartesian geometry.

2. THE SINGULAR CHARACTERISTIC TRACKING ALGORITHM AND ITS IMPLEMENTATION

The error in standard algorithms for solving the DO transport equation is primarily due to the smearing of edge values across the SC. The description of the smearing effect case of uncollided flux has been reported in [7], which follows from the local error analysis performed in [4]. The local error analysis shows that, in the limit of diminishing cell size with fixed *optical aspect ratio,* $\xi = \eta a / \mu b$ (a cell width, b cell height), the error in the average angular flux for Diamond Difference (DD) is given by

$$error \rightarrow \left| \frac{\xi(1-\xi)}{2(1+\xi)}\psi_B - \frac{\xi(1-\xi)}{2(1+\xi)}\psi_L + O(a,b) \right|$$

which reveals that in case the locally exact incoming fluxes, ψ_{B} and ψ_{L} are not equal, the error will not diminish with mesh refinement unless $\xi = 1$. The more general result for all WDD is given in [4]. Then, the SCT algorithm proposes to split cells traversed by the SC along its direction and to solve the Step Characteristics [9] equations separately on each side ("A", "B") of the intersected cells as shown in Fig. 1. Thus, whenever a cell containing an SC is being *swept*, the partial average outgoing edge fluxes on each side of the SC (corresponding to the thick edges in Fig. 1) are computed separately, in terms of the partial incoming-edge fluxes and the cell volumetric source and they are stored individually. The intersection point of the SC with the exiting edge is also computed and used to determine the next cell in the sweep sequence that contains the SC. The remaining cells are solved using the standard Diamond Difference method, or any other standard method for that matter.

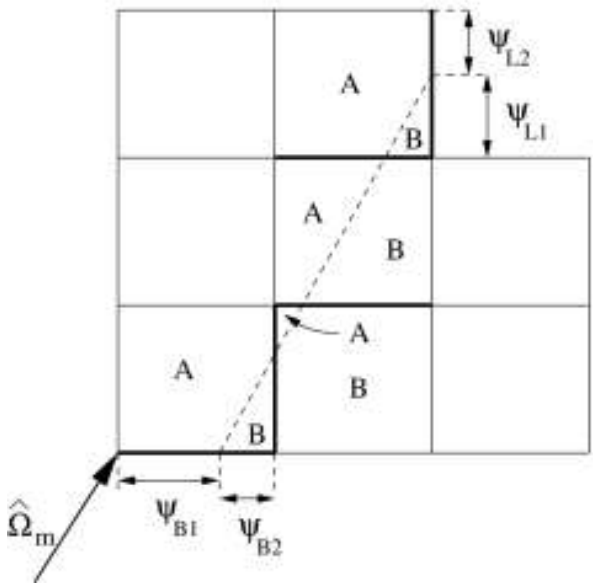

Figure. 1. Schematic diagram of a group of cells that shows the partial incoming fluxes on each side of the SC (dotted line) for a discrete ordinate in the positive quadrant. The SCT algorithm only modifies the computations in cells traversed by the SC.

2.1. Implementation

The SCT algorithm is implemented in a steady state, two-dimensional Cartesian geometry, monoenergetic, S_N test-code using the standard inner iterations [10] to resolve the scattering source. In the Discrete Ordinates equations, a SC emanates form every corner of the domain for each incoming angular flux. These lines, across which the angular flux can present varying degrees of discontinuity, are specifically defined with an example in Section 4.1.

Using the rotation and inversion of coordinate axes employed in defining the sweep algorithm allows us to consider only angles in the positive quadrant. For these angles, three cases of intersection of the SC with the outgoing edges of the cell under consideration are possible when $b/\eta \le a/\mu$. These *cases* are illustrated in Fig. 2, where the incoming fluxes on both sides of the SC are depicted schematically for each case. For the "case 1" intersection the incoming fluxes are ψ_{B}, ψ_{L1} and ψ_{L2} and the equations are:

$\psi_{\mathrm{L}} = \psi_{\mathrm{L1}}\tau_L + \psi_{\mathrm{L2}}(1-\tau_L)$: average left incoming angular flux, ψ_{T1}

$\psi_{\mathrm{R}} = (\psi_{\mathrm{B}} - q_{scat})\dfrac{1-e^{-\varepsilon_y}}{\varepsilon_y} + q_{scat}$: average right outgoing angular flux.

$\psi_{\mathrm{T1}} = (\psi_{\mathrm{L2}} - q_{scat})\dfrac{1-e^{-\tau_L\varepsilon_y}}{\tau_L\varepsilon_y} + q_{scat}$: top left outgoing angular flux, and $\varepsilon_y = \dfrac{2b}{\eta}$, $\varepsilon_x = \dfrac{2a}{\eta}$,

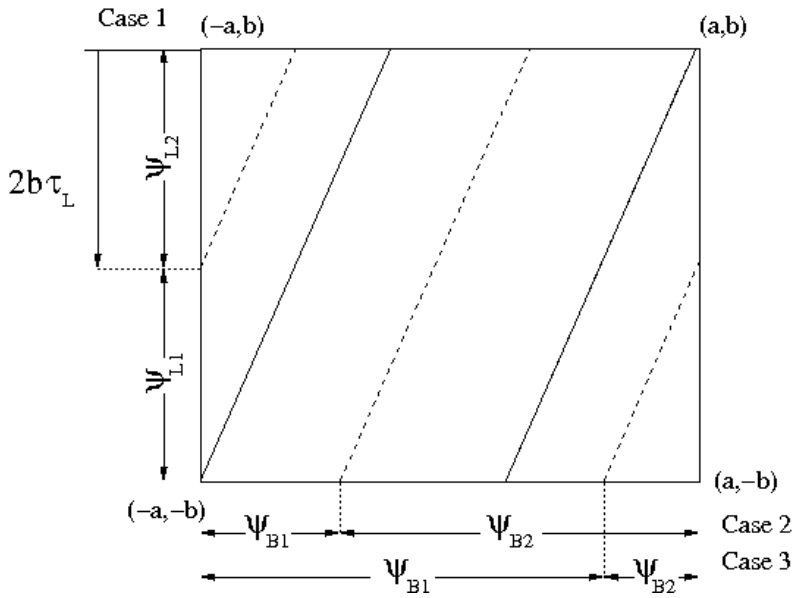

Figure. 2. Diagram of a cell that shows the definition of the partial incoming fluxes on each side of the SC (dotted lines) for each of the three possible cases for $\mu > 0, \eta > 0$ and $b/\eta < a/\mu$, in the SCT algorithm. The intersection, $2b\,\tau_L$, for case 1 is also shown.

$$\psi_{T2} = \left(\psi_B e^{-\varepsilon_y} + q_{scat}(1-e^{-\varepsilon_y})\right)\frac{1-\xi}{1-\xi\tau_L} + \left((\psi_{L1} - q_{scat})\frac{e^{(1-\tau_L)\varepsilon_y}-1}{(1-\tau_L)\varepsilon_y} + q_{scat}\right)\frac{\xi(1-\tau_L)}{1-\xi\tau_L}$$: top right

outgoing angular flux,

$\psi_T = \psi_{T1}\xi\tau_L + \psi_{T2}(1-\xi\tau_L)$: average top outgoing angular flux.

Notice ψ_T is not used downstream, but ψ_{T1} and ψ_{T2} are used instead in the next cell calculation. The balance equation is used to compute the average angular flux, which in turn is used to update the scattering terms.

$$\overline{\psi} = \frac{\psi_R - \psi_L}{\varepsilon_x} + \frac{\psi_T - \psi_B}{\varepsilon_x} - \frac{q_{scat}}{\sigma}$$

$$q_{scat} = \sigma_s \sum_{n=1}^{N} w_n \overline{\psi} + \overline{Q}$$

Analogous expressions apply for cases 2 and 3 with suitable intersection coordinates for the SC intersection with the edges. The remaining intersection cases (i.e. intersection for $b/\eta > a/\mu$) are resolved via a corresponding case from the three cases depicted in Fig. 2 using a mesh transposition.

In summary, the SCT algorithm is based on the step characteristic equations solved on each side of the SC in order to avoid smearing the contributions of the outgoing fluxes into a single outgoing-edge value. The separate computation of the edge flux variables on each side of the SC results in pointwise convergence of the numerical solution to the exact solution in the case of discontinuous exact flux across the SC without scattering as reported in[6].

3. METHOD OF MANUFACTURED SOLUTIONS

Given the lack of analytical solutions for the transport problem with scattering in *x*,*y* geometry, the Method of Manufactured Solution (MMS) (first proposed in [11]) was deployed to generate exact reference solutions. These are necessary to test the ability of our new algorithm to accurately compute flux solutions with different levels of discontinuity in the flux itself or its first derivatives, and to compare its performance with respect to standard numerical methods.

Ad hoc analytical solutions are proposed following the MMS procedure from which an external source and appropriate boundary conditions are devised using the spatially undiscretized Discrete Ordinates equations. A key concept on which MMS is founded is that for code verification purposes the proposed solution, sources and boundary conditions need not be physically realizable. On the other hand, it is desirable that the solution has sufficiently complex features to test the numerical approximation of all the terms in the target equation.

In the MMS method [12], a reference solution specified by an analytical expression is generated by proposing a mathematical formula for the angular flux $\psi(\vec{x},\hat{\Omega}_i)$ and introducing it into the Discrete Ordinates equations, Eq. (1), to generate an external source per discrete ordinate

$$Q(\vec{x},\hat{\Omega}_i) = \hat{\Omega}_i \cdot \nabla\psi(\vec{x},\hat{\Omega}_i) + \sigma(\vec{x})\psi(\vec{x},\hat{\Omega}_i) - \sum_{n=1}^{N} w_n \sigma_s(\vec{x},\hat{\Omega}_i,\hat{\Omega}_n)\psi(\vec{x},\hat{\Omega}_n) \qquad (2.a)$$

The appropriate boundary conditions for the incoming angular flux are also set by evaluating the prescribed analytical solution for incoming discrete ordinates on the boundaries of the problem domain, Γ:

$$\psi(\vec{x},\hat{\Omega}_i) = \psi(\vec{x},\hat{\Omega}_i) \quad \text{for } \vec{x} \in \Gamma \text{ and } \hat{\Omega}_i \cdot \hat{n} < 0 \qquad (2.b)$$

where $\hat{n}$ is the outward normal at the boundary point *x*. If the DO transport equations were solved using the distributed source specified in Eq. (2.a) and the boundary conditions in Eq. (2.b) with no spatial discretization error the numerical solution, $\psi(\vec{x},\hat{\Omega}_i)$, would be identical to the proposed analytical solution, $\psi(\vec{x},\hat{\Omega}_i)$. Hence the convergence of ψ to ψ with mesh refinement characterizes the accuracy of the underlying numerical method.

4. IMPROVED RATE OF CONVERGENCE

Comparison of the accuracy of s*tandard* WWD methods for solving the discrete ordinates equations and the SCT algorithm is conducted via numerical experiments on a domain comprised of a square of dimensions 1.0 *mfp* × 1.0 *mfp*. The material composition is homogeneous with scattering ratio equal to ½. The square is divided into $2^n \times 2^n$ mesh, n=0,...,12, and the error in each computational cell is computed as $|\overline{\Phi} - \overline{\phi}|$, where $\overline{\Phi}$ and $\overline{\phi}$ are the numerical and exact cell-average scalar fluxes, respectively, computed as the integral of the scalar flux over a computational cell divided by the cell's area. Notice that the numerical and exact scalar fluxes are computed using a given angular quadrature. Therefore, the error computed is entirely due to the spatial discretization and not to angular discretization since the reference solution, ϕ has the

same angular discretization as the numerical solution, Φ. The problems presented are solved with Level Symmetric S_4 and S_8 quadratures [10].

Results of the new algorithm are compared with the standard codes for the DD method and linear spatial approximation order of the Arbitrarily High Order Transport method of the Nodal type (AHOT-N1) [3] using two test problems.

4.1. Solution with Flux Discontinuity

The chosen analytical solution for the case with discontinuous flux is the solution of the uncollided flux for external boundary source in one and only one given discrete direction. The incoming flux along all other discrete ordinates and problem boundaries is set to zero. The exact angular flux is given for the first quadrant angle by,

$$\psi(x,y) = \begin{cases} \psi_L e^{-\sigma x/\mu}, & y > x\dfrac{\eta}{\mu} \\ \psi_B e^{-\sigma y/\eta}, & y < x\dfrac{\eta}{\mu} \end{cases} \tag{3}$$

where ψ_L and ψ_B are constants that define the incoming fluxes on the left and bottom edges of the square problem domain, and $\mu>0$ and $\eta>0$ are the direction cosines of the discrete ordinate with respect to the x- and y-axes, respectively, and σ is the total macroscopic cross section. The solution is not defined along the Singular Characteristic (SC), $y = x\eta/\mu$, since, in general, the flux ψ could experience a discontinuity across the SC, as is the case for unequal incoming fluxes ψ_L and ψ_B. In the specific test problem whose solution error norms are depicted in Fig. 3, μ = 0.3500212, η= 0.8688903, ψ_L =1/2 and ψ_B =1.

Figure 3 shows that the standard algorithms do not convergence in L_∞ error norm. Although, the slopes of these curves are negative in the numerical results, it is simple to prove that, since the algorithms preserve local balance of particles, the solutions cannot diverge. Therefore, the

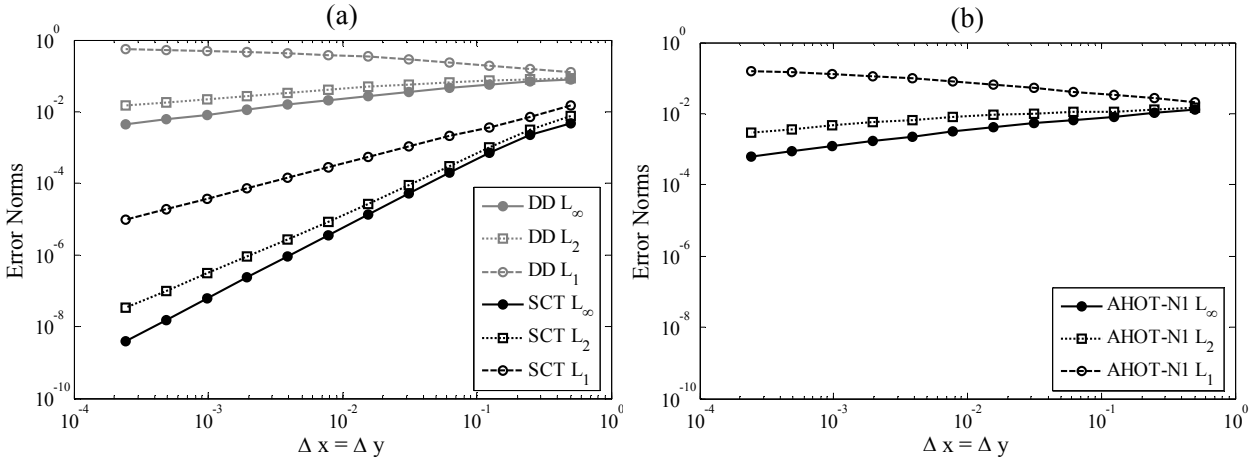

Figure 3. Error norms for the (a) DD and SCT and (b) AHOT-N1 methods with respect to the MMS solution with discontinuity (S_4 quadrature)..

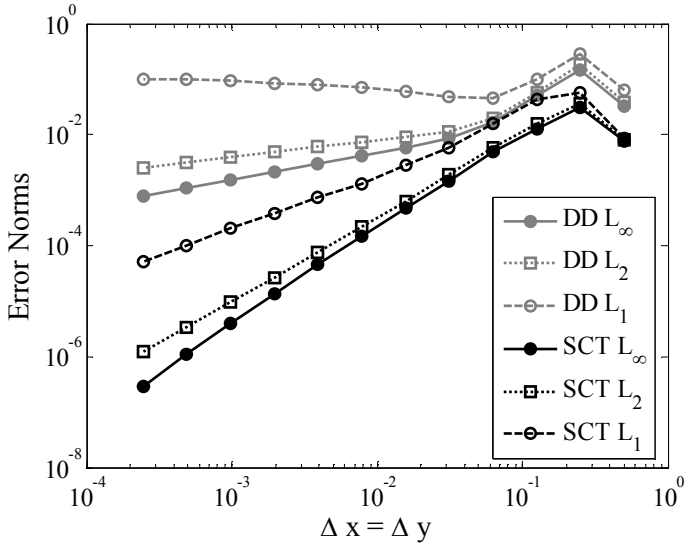

Figure 4. Error Norms are plotted for the standard (DD) and modified method (SCT) for a solution with flux discontinuity and absolute positive source (S_8 quadrature).

correct asymptotic rates of convergence for the standard methods' error L_∞ norm are zero, which they seem to approach asymptotically with diminishing cell size. In contrast, the SCT method's error L_∞ norm, also shown in Fig. 3, diminishes with mesh refinement, and SCT also significantly decreases the magnitude of the error with higher rates of convergence for the integral norms L_1 and L_2 (see Table I).

By substituting Eq. (3) into Eq. (2.a), it becomes immediately apparent that $Q(\vec{x},\hat{\Omega}_i)$ is negative throughout the problem domain since the first two terms on the right hand side cancel each other and the last term is definitely negative. To rule out any adverse influence the negative source might have on the non-convergence feature of the L_∞ norm, we devised a positive source problem with discontinuous flux exact solution. To achieve this, we summed the source described in Section 4.2 below and the negative source described above, yielding a positive source. The results of the DD and SCT methods shown in Fig. 4 continue to exhibit lack of solution pointwise convergence of the former, implying that the discontinuity of the flux is the cause of this undesirable behavior of the DD method.

4.2. Solution with Discontinuous Derivatives

The analytical solution with discontinuous derivatives is the analytical uncollided flux solution of the DO equations with uniform source, $q = 1$, and vacuum boundary conditions. For an angle in the first quadrant the expression of the angular flux is

$$\psi(x,y) = \begin{cases} \dfrac{q}{\sigma}(1-e^{-\sigma x/\mu}), & y > x\dfrac{\eta}{\mu} \\ \dfrac{q}{\sigma}(1-e^{-\sigma y/\eta}), & y < x\dfrac{\eta}{\mu} \end{cases} \tag{4}$$

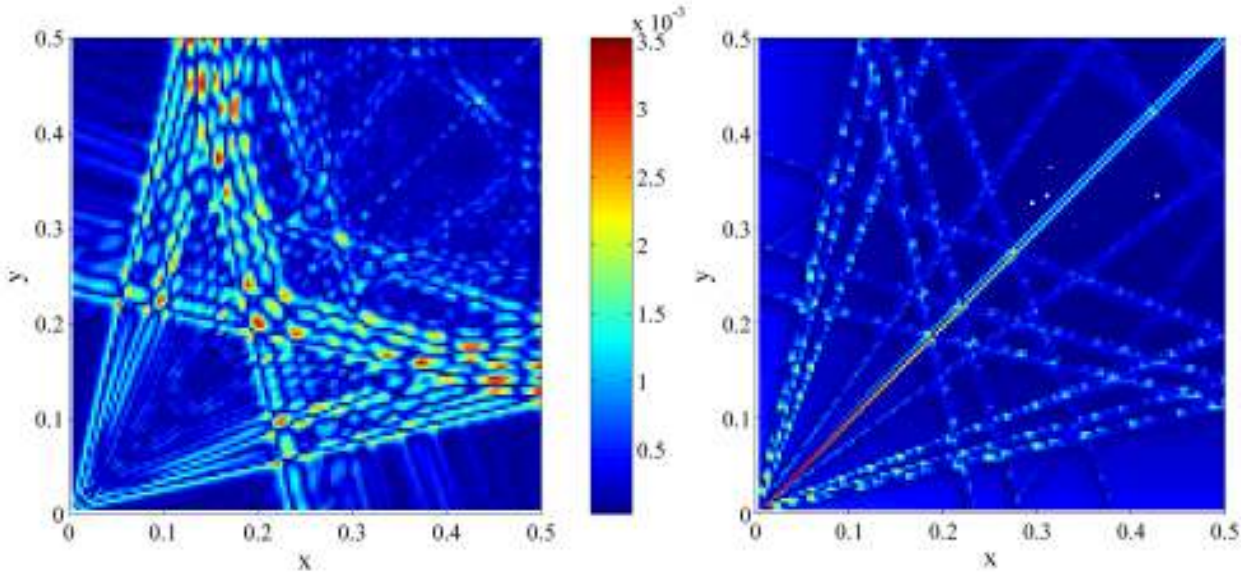

Figure 5. Scalar flux error pattern for the DD (Left) and the SCT (Right) (with scale × 0.2) methods with respect to the MMS solution with discontinuous derivatives. One fourth of the symmetric domain is shown; $\Delta x = \Delta y = 3.9\ 10^{-3}$ *mfp*, S_8 quadrature.

The corresponding scalar flux is the result of the quadrature sum of the angular fluxes for all discrete angles in all quadrants with expressions analogous to Eq. (4).

In Fig. 5, the solution errors using DD and SCT are shown for comparison for the problem using Level Symmetric S_8 quadrature. The error pattern reveals the SC lines where the discretization of the spatial variable fails to reproduce the discontinuities of the derivatives in the flux. The pattern is not due to ray effects since the source is uniformly distributed. The discontinuity of the derivative produces strong wiggles in the DD solution while in the new SCT code the error is a factor of 5 smaller and is largely confined to a tight neighborhood near the SC lines.

The L_∞, L_2 and L_1 error norms of the DD, SCT and AHOT-N1 solutions for this problem are shown in Fig. 6 and Table I. Figure 6(a) shows that SCT increases the rate of convergence with respect to DD. Comparison with the results in Fig. 6(b) reveals that SCT achieves comparable rates of convergence and error magnitudes to those obtained with AHOT-N1 for the same level of mesh discretization. Nonetheless, a fairer comparison between the two methods is provided by Fig 7. The error level of the latter two methods, SCT and AHOT-N1 are compared as a function of the degrees of freedom or number of discrete variable unknowns solved for. Figure 7 shows that SCT performs better that AHOT-N1 for the same number of unknowns. Since the SCT does not excessively increase the computational load compared to the original DD method, the overall computational cost is decreased, relative to AHOT-N1, for the same level of error.

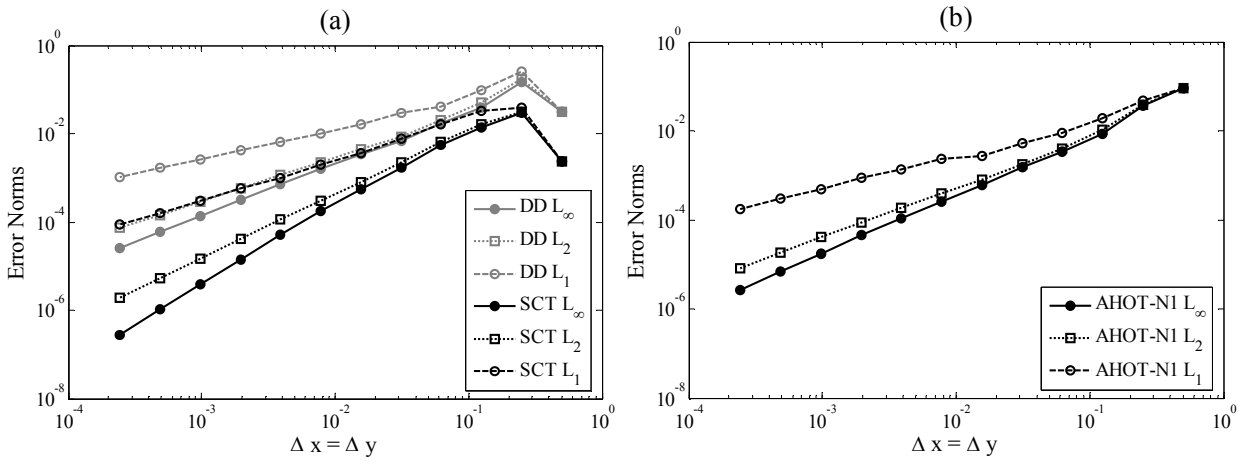

Figure 6. Error norms for the (a) DD and SCT and (b) AHOT-N1 methods with respect to the MMS solution with discontinuous derivatives (S_4 quadrature).

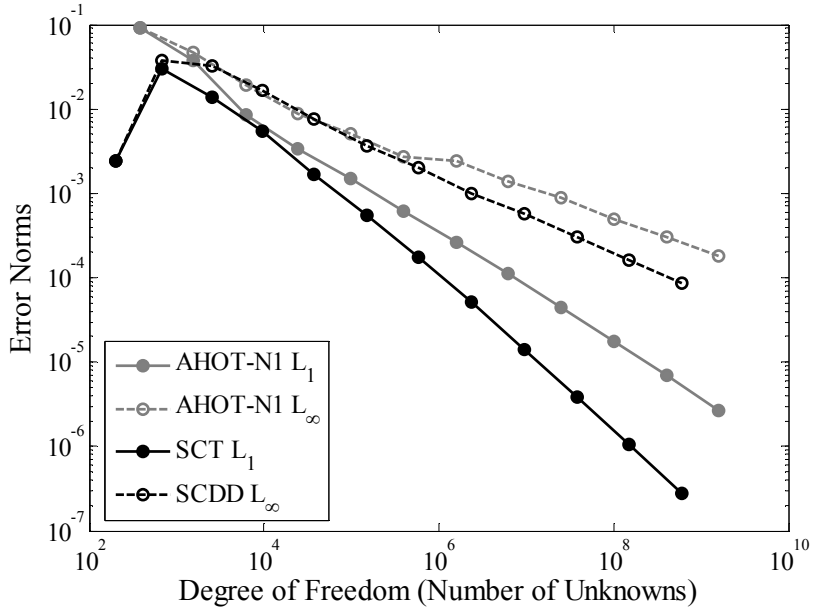

Figure 7. The L_∞ and L_1 error norms plot for the AHOT-N1 and SCT methods with respect to the MMS solution with discontinuous derivatives. The error is shown as a function of degrees of freedom. The SCT method clearly performs better than AHOT-N1 for the same number of unknowns (S_4 quadrature).

5. CONCLUSION

A simple and effective modification to existing numerical methods for solving the discrete ordinates equations that restores their theoretical order of convergence in the L_1 error norm in the case of discontinuous flux has been devised. More importantly, the method yields solutions that converge pointwise to the exact solution with mesh refinement for cases where the standard methods do not converge. Specifically, these are configurations where the exact solution undergoes a discontinuity across the SC.

The new algorithm was also tested using the manufactured solution proposed in [5], results not presented in this paper. That particular reference solution has all spatial partial derivative defined/bounded everywhere. In this case, the tested algorithms attain their theoretical rate of convergence determined by the order of the discretization stencil. On the other hand, it was noted in the past [2] that a solution with bounded third partial derivatives is too smooth a constraint for most applications. While a discontinuous angular flux solution can be considered as a *worst case scenario* which bounds the minimum achievable rate of convergence, a more realistic class of solutions exhibits some degree of discontinuity in the first derivatives for which the SCT algorithm produces accurate results at a low computational cost.

Table I. Rate of convergence: comparison between standard DD, AHOT-N1 and the new SCT methods.

Angular Flux Solution		**Discontinuous** (negative source)		**Discontinuous Derivative**	
Method	**Error Norm**	**Standard**	**SCT**	**Standard**	**SCT**
DD	L_1	0.47	1.97	1.24	1.93
	L_2	0.31	1.57	1.00	1.48
	L_∞	-0.07	0.99	0.66	0.92
AHOT-N1	L_1	0.48		1.38	
	L_2	0.32		1.15	
	L_∞	-0.14		0.79	

REFERENCES

1. J. Arkuszewski, "Rigorous Analysis of the Diamond Approximation for the Neutron Transport Equation", *Numerical Reactor Calculations*, **STI/PUB/307**, 113, International Atomic Agency, (1972).
2. J. Arkuszewski, "Effect of Singularities on Approximations in S_N Methods", *Nucl. Sci. Eng.*, **49**, pp. 20-26, (1972).
3. Y. Y. Azmy, "The Weighted Diamond Difference Form of Nodal Transport Methods", *Nucl. Sci. Eng.*, **98**, 29 (1988).
4. Y. Y. Azmy, "Local Accuracy of Weighted Diamond Difference Schemes", *Trans. Am. Nucl. Soc.* **83**, 433, (2000).
5. C. Drumm, "Manufactured Solution Verification of the Ceptre code", (Personal Communication) (2006).
6. J. I. Duo, J. I., Y. Y. Azmy, "Discrete Ordinates Singular Characteristic Tracking Algorithm", *Proc. of the ANS Winter National Meeting*, Washington, November 13-17, (2005).
7. J. I. Duo, Y. Y. Azmy, "Error Comparison of Diamond Difference, Nodal and Characteristics Methods for Solving Multidimensional Transport Problems with the Discrete Ordinates Approximation", *Nucl. Sci. Eng.*, (Accepted for Publication September 6, 2006, to appear in June 2007 issue).
8. E. W. Larsen, "Spatial Convergence Properties of the DD Method in *x*,*y* Geometry, *Nucl. Sci. Eng.*, **80**, 710, (1982).
9. K. D. Lathrop, "Spatial Differencing of the Transport Equation: Positivity vs. Accuracy", *Comp. Phys.*, **4**, pp. 475-498 (1969).
10. E. E. Lewis, W. F. Miller, *Computational Methods of Neutron Transport*, John Wiley & Sons, New York, United States (1984).
11. C. Lingus, "Analytical Test Cases for Neutron and Radiation Transport Codes", *Proc. Second Conference on Transport Theory*, Jan 26-29, 1971, Los Alamos, New Mexico, U.S. Atomic Energy Commission, CONF-710017 (1971).
12. P. J. Roache, "Code Verification by the Method of Manufactured Solutions", ASME J. Fluids Eng., **124**, No. 1, Mar., pp. 4-10 (2002).